

# INFLUENCE OF TEMPERING TEMPERATURE ON MECHANICAL PROPERTIES OF ULTRA-HIGH STRENGTH LOW-ALLOY STEELS

Jana Horníková, Pavel Šandera, Jaroslav Pokluda  
Brno University of Technology, Czech Republic

## ABSTRACT

The results of both the experimental investigation and the literary survey on the role of the tempering temperature within a wide range of mechanical properties is presented for selected ultra-high strength low alloy (UHSLA) steels of American (AISI 4340, 300M and Garrison NiSiCr) and Czech (P-LDHA and V-ROL N) provenance. The analysis confirmed the equivalence of steels 300 M and P-LDHA and their superiority among investigated steels. The optimum tempering temperature was proved to be 300 °C for prevailing majority of mechanical characteristics of all steels. The only exception is the steel V ROL N, where the optimum temperature is shifted down to 200 °C.

## KEYWORDS

Ultra-high strength low-alloy steels, mechanical properties, tempering temperature, heat treatment, ratcheting, fatigue life

## INTRODUCTION

Ultra-high strength steels of the yield strength above 1400 MPa are developing for more than 40 years. They can be divided into the following categories [1–3]; low alloy martensitic steels (UHSLA), maraging steels, high alloy secondary hardened steels and precipitation hardened steels. UHSLA steels are the most effective, commercially used, materials for strongly exposed components in the aircraft and atomic power industry. The classical steel AISI 4340 is still the most popular representative of that category. Starting from 1960 the 300M steel (the AISI 4340 modified by much higher content of Si) is preferentially used in the US military industry. The steel P-LDHA, the Czech equivalent of the 300M steel, was developed in the early 1990's to replace the high strength steel V-ROL N in military applications. Also Garrison NiSiCr steels are commonly used in practice.

It is well known that the optimal heat treatment for achievement of best standard tensile properties, hardness and the endurance limit of UHSLA steels consists of quenching in the range of 845 – 900 °C and tempering in the range of 250 – 300 °C, in dependence on the chemical composition [4] (see Tab. 1). Minimum acceptable values of tensile properties of selected UHSLA steels are displayed in Tab. 2.

Because of an extended use of UHSLA steels in extreme loading conditions in the last 10 years, also the heat-treatment optimization of other special mechanical properties is of a great importance. This paper presents experimental results of long term investigation focused on the influence of tempering temperature on fracture toughness, absorbed energy (notch toughness), low cycle fatigue life, stress ratio effect, notch sensitivity and cyclic creep resistance of the P-LDHA and V-ROL N steels. Results are discussed in terms of microstructure conditions obtained after different heat

treatments. Moreover, comparison with other steels as the ultra-high strength AISI 4340, Garrison NiSiCr steel or the 300M steel is performed in a wide range of standard and special mechanical properties.

TAB. 1. Chemical composition of some UHSLA steels.

| Steel     | C         | Mn        | Si        | Cr        | Ni        | Mo        | V         |
|-----------|-----------|-----------|-----------|-----------|-----------|-----------|-----------|
| AISI 4340 | 0,38–0,43 | 0,60–0,80 | 0,20–0,35 | 0,70–0,90 | 1,65–2,00 | 0,20–0,30 | 0,05–0,10 |
| 300M,     | 0,40–0,46 | 0,65–0,90 | 1,45–1,80 | 0,70–0,95 | 1,65–2,00 | 0,30–0,45 | —         |
| P-LDHA    |           |           |           |           |           |           |           |
| NiSiCr    | 0,34      | 0,46      | 1,88      | 1,02      | 2,89      | —         | —         |

TAB. 2. Minimum values of tensile properties (yield stress  $\sigma_y$ , ultimate stress  $\sigma_u$ , elongation  $\delta_5$  and contraction  $\psi$ ) for selected UHSLA steels.

| Steel         |        | $\sigma_y$<br>[MPa] | $\sigma_u$<br>[MPa] | $\delta_5$<br>[%] | $\psi$<br>[%] |
|---------------|--------|---------------------|---------------------|-------------------|---------------|
| AISI 4340     | [5, 6] | 1496                | 1793                | 10                | 43            |
| 300M (0,40 C) | [6]    | 1517                | 1862                | 8                 | 27            |
| 300M (0,42 C) | [6]    | 1586                | 1931                | 7                 | 25            |
| D6ac          | [6]    | 1476                | 1768                | 11                | 45            |
| 30ChGSN2A     | [7]    | 1373                | 1619                | 9                 | 45            |
| ROL N         | [8]    | 1350                | 1570                | 9                 | 40            |
| P-LDHA        | [9]    | 1580                | 1930                | 7                 | 25            |

## 1. INFLUENCE OF TEMPERING TEMPERATURE ON MICROSTRUCTURE

The microstructural analysis of the steel P-LDHA can serve as a typical example of microstructural changes caused by various tempering temperatures. The result of metallographical investigation is depicted in Fig. 1. The microstructure of the as-received sample (quenching and high-temperature annealing) corresponds to the high-tempered martensite-bainite microstructure containing coarse carbides. The microstructures after quenching and tempering at  $T_t = 200^\circ\text{C}$  and  $T_t = 300^\circ\text{C}$  become generally finer and correspond to a low-tempered martensite. The structure of the medium-tempered martensite at  $T_t = 400^\circ\text{C}$  corresponds to the range of tempering-embrittlement caused by interlath cementite precipitation. In this microstructure, a partial transformation of the  $\varepsilon$ -carbide to the cementite  $\text{Fe}_3\text{C}$  can be anticipated. The high-temperature tempering at  $T_t = 670^\circ\text{C}$  practically finishes the transformation  $\varepsilon \rightarrow \text{Fe}_3\text{C}$ . The changes in the carbide shape and its content can be very clearly seen from two-step biodeen-carbon replicas observed in the transmission electron microscope (Fig. 2). In the low-tempered microstructures, the matrix is oversaturated and strengthened by carbon. In the high-tempered microstructure, on the other hand, practically all carbon constitutes a part of coarse carbides and, therefore, the strength of the matrix becomes much lower. There is, however, an important microstructural process, invisible on Figs. 1 and 2, running particularly in

the temperature range  $T_t \in \langle 350, 500 \rangle$  °C. Namely, the precipitation of interlath carbides evoked by the decay of retained austenite films. It is the main reason for the tempering embrittlement. The start of this process at  $T_t = 350$  °C can be deduced from the break of the curves of retained austenite volume fraction in Fig. 3, measured by means of the X-ray diffraction [10]. All the above mentioned microstructural changes substantially determine the resulting mechanical properties of UHSLA steels.

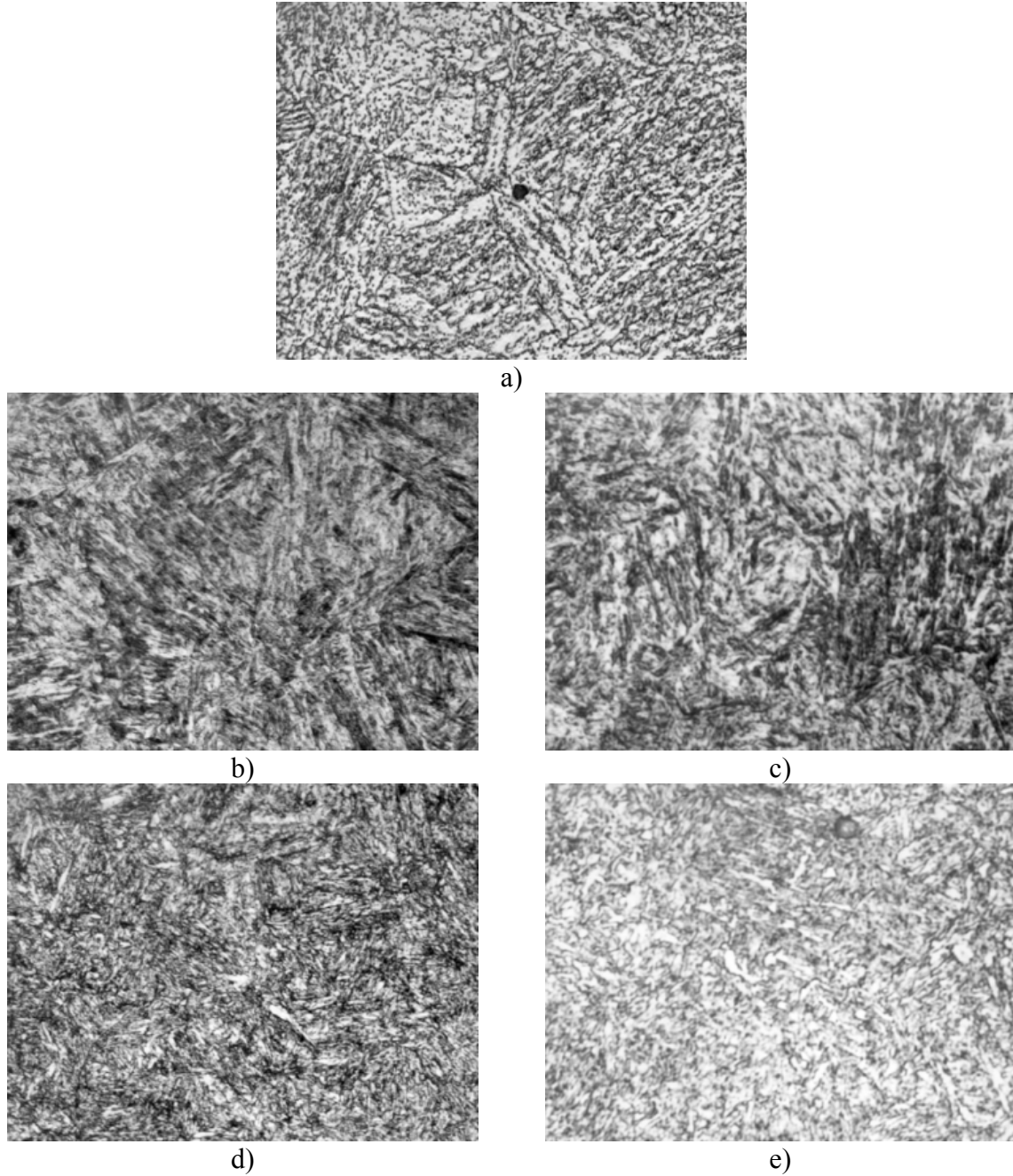


Fig. 1: Influence of the tempering temperature on the microstructure of P-LDHA steel (metallographical samples). a) as-received, b)  $T_t = 200$  °C, c)  $T_t = 300$  °C, d)  $T_t = 400$  °C, e)  $T_t = 670$  °C,

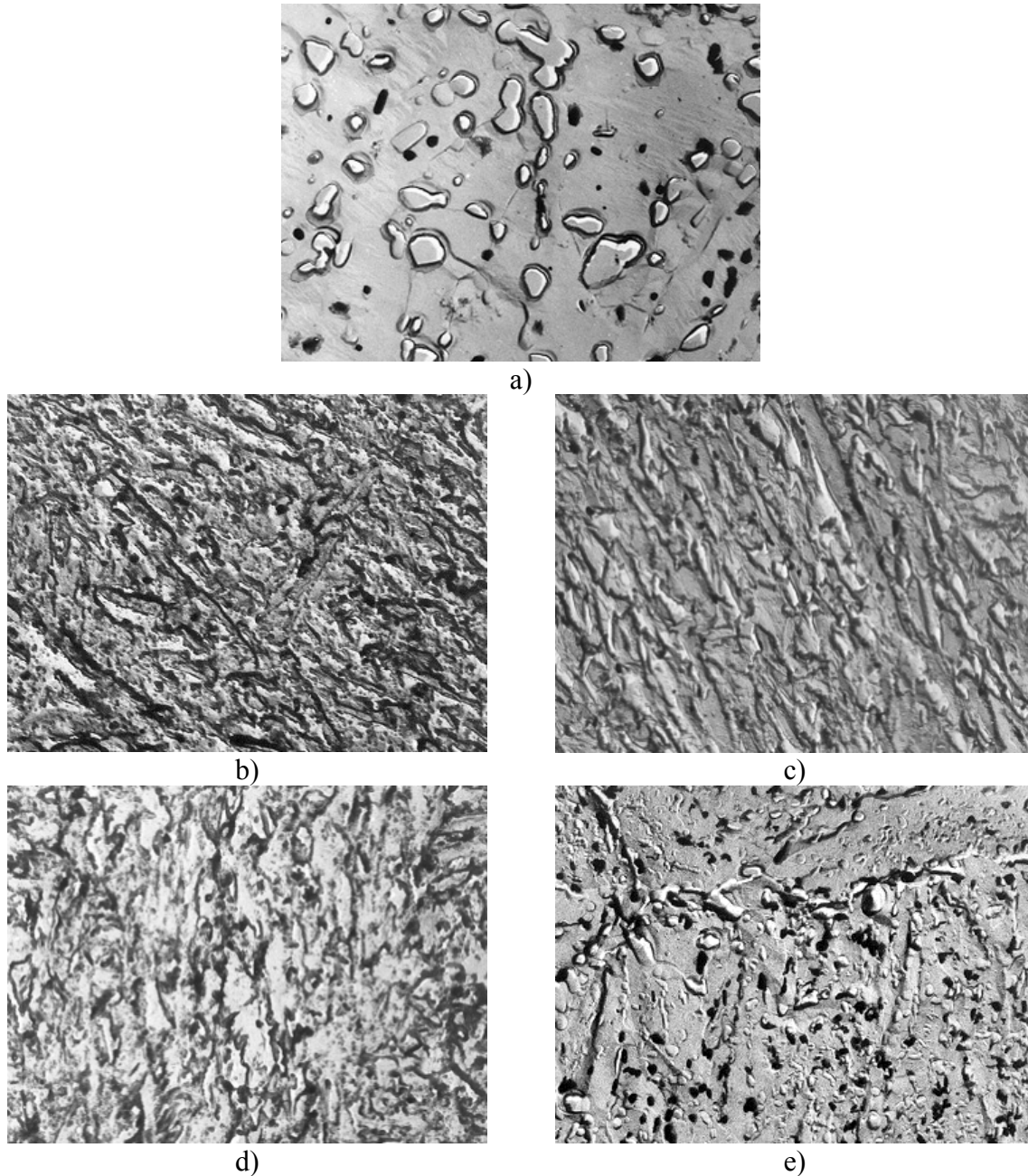


Fig. 2: Influence of the tempering temperature on the carbide content in the P-LDHA steel (TEM biodecarbon replicas). a) as-received, b)  $T_t = 200\text{ }^{\circ}\text{C}$ , c)  $T_t = 300\text{ }^{\circ}\text{C}$ , d)  $T_t = 400\text{ }^{\circ}\text{C}$ , e)  $T_t = 670\text{ }^{\circ}\text{C}$ ,

## 2. INFLUENCE OF TEMPERING TEMPERATURE ON MECHANICAL PROPERTIES

The curves in Figs. 4 – 8 represent an average mechanical response of various UHSLA steels to the changing tempering temperature [10–12]. A steep drop in the yield stress can be observed with increasing temperature after reaching  $T_t \approx 350\text{ }^{\circ}\text{C}$ . This is associated with a rather moderate increase in the ductility. However, in the range of  $T_t \in \langle 350, 550 \rangle\text{ }^{\circ}\text{C}$ , local minima of both the absorbed energy and the fracture toughness indicate a dangerous embrittlement of the material. One can clearly see that, with respect to an average of mechanical properties, the optimum tempering temperature lies in the range of  $T_t \in \langle 250, 310 \rangle\text{ }^{\circ}\text{C}$ .

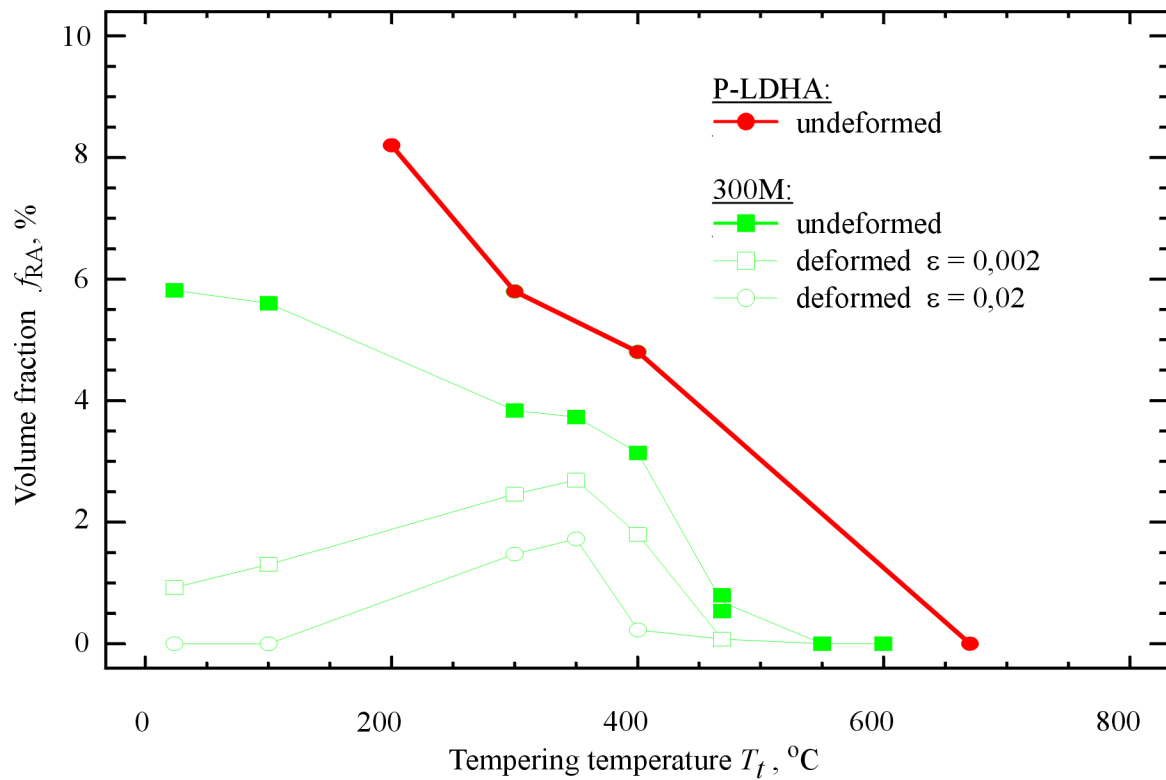


Fig. 3: The volume fraction of the retained austenite as function of the tempering temperature in steels 300M and P-LDHA.

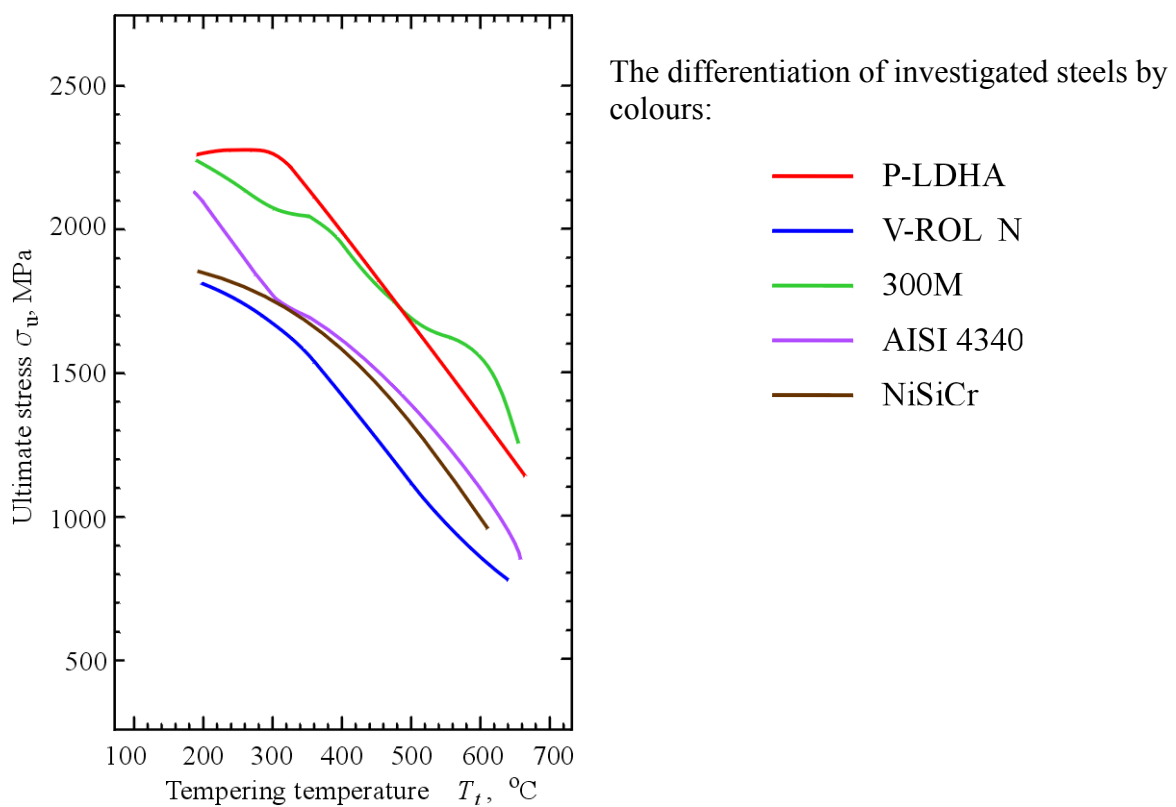


Fig. 4: The ultimate stress as function of the tempering temperature

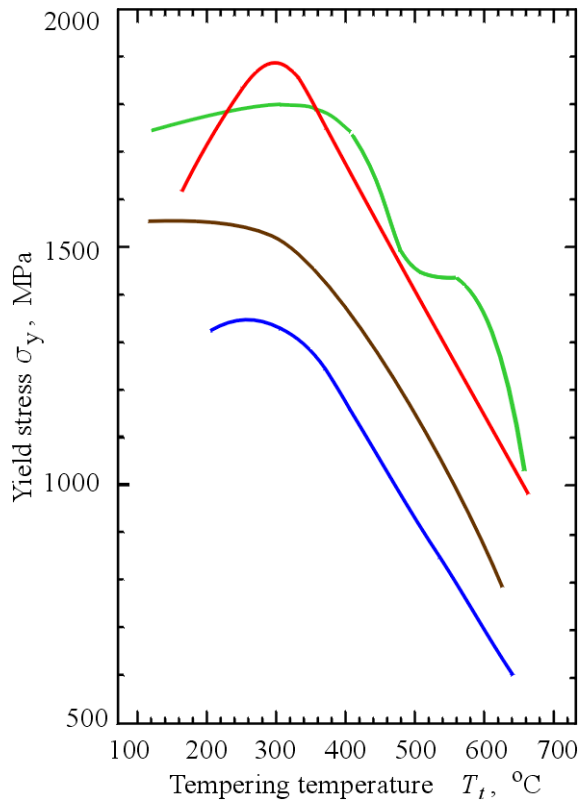


Fig. 5: The yield stress as function of the tempering temperature

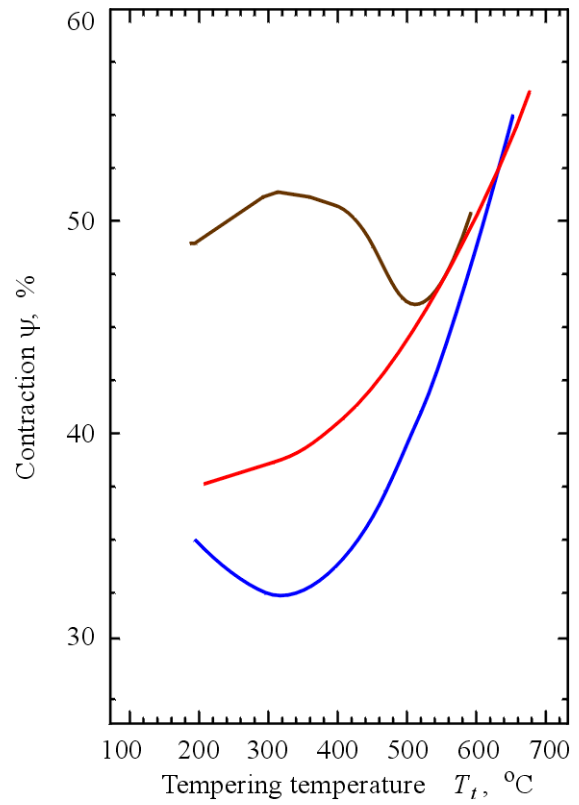


Fig. 6: The contraction as function of the tempering temperature

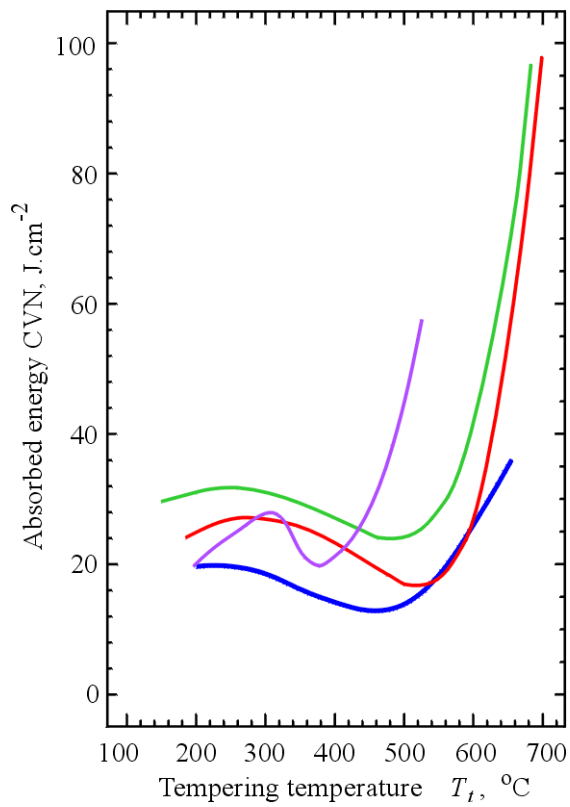


Fig. 7: The absorbed energy as function of the tempering temperature

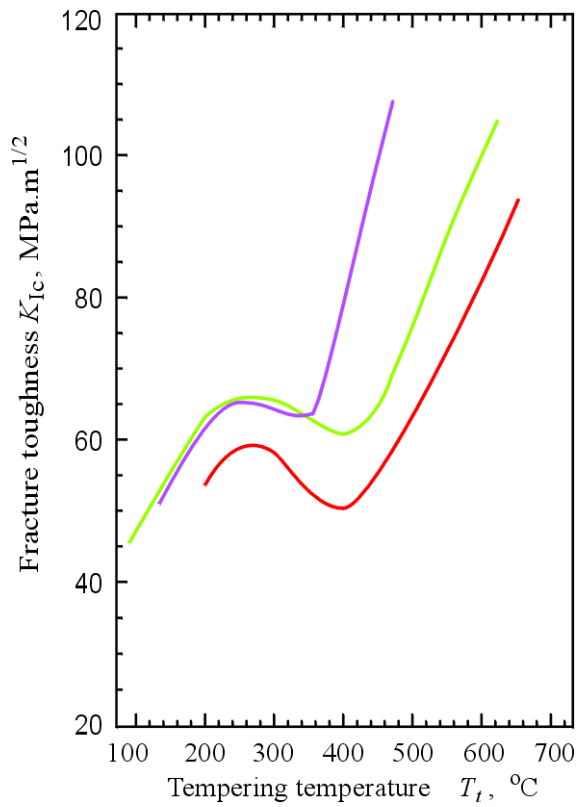


Fig. 8: The fracture toughness as function of the tempering temperature

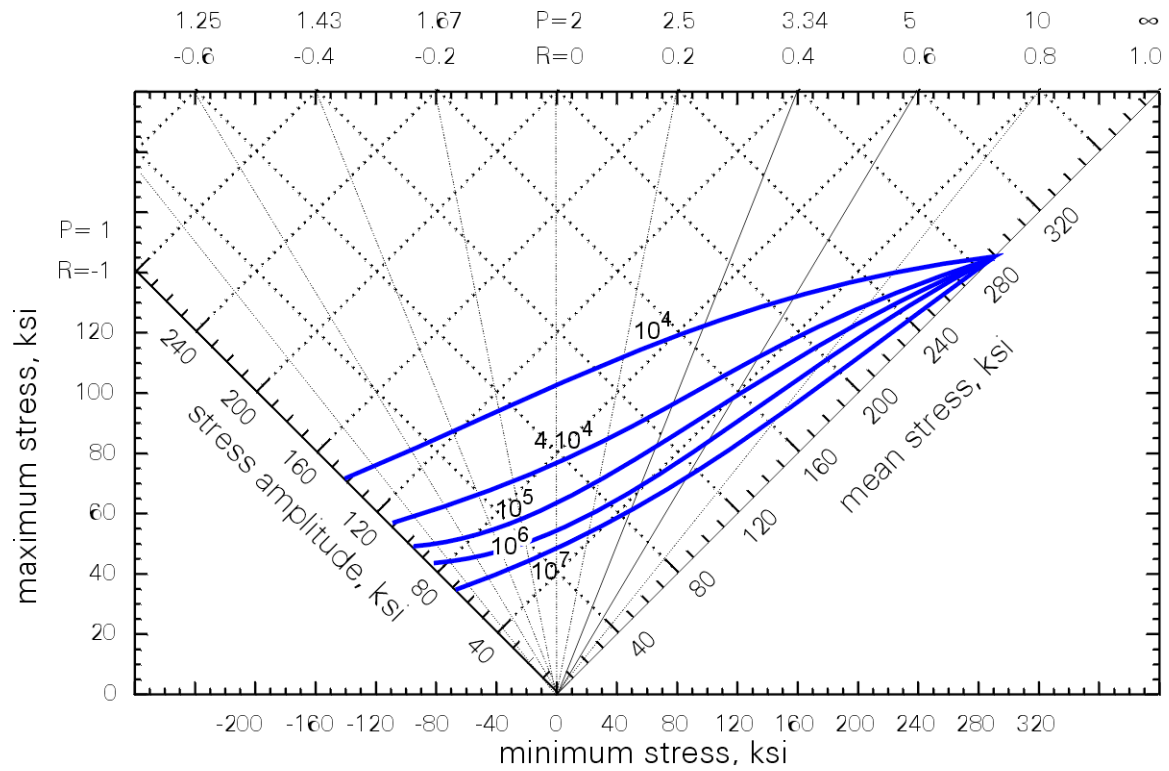


Fig. 9: The fatigue constant-life diagram for the V-ROL N steel (smooth specimens)  
1 ksi = 6.895 MPa.

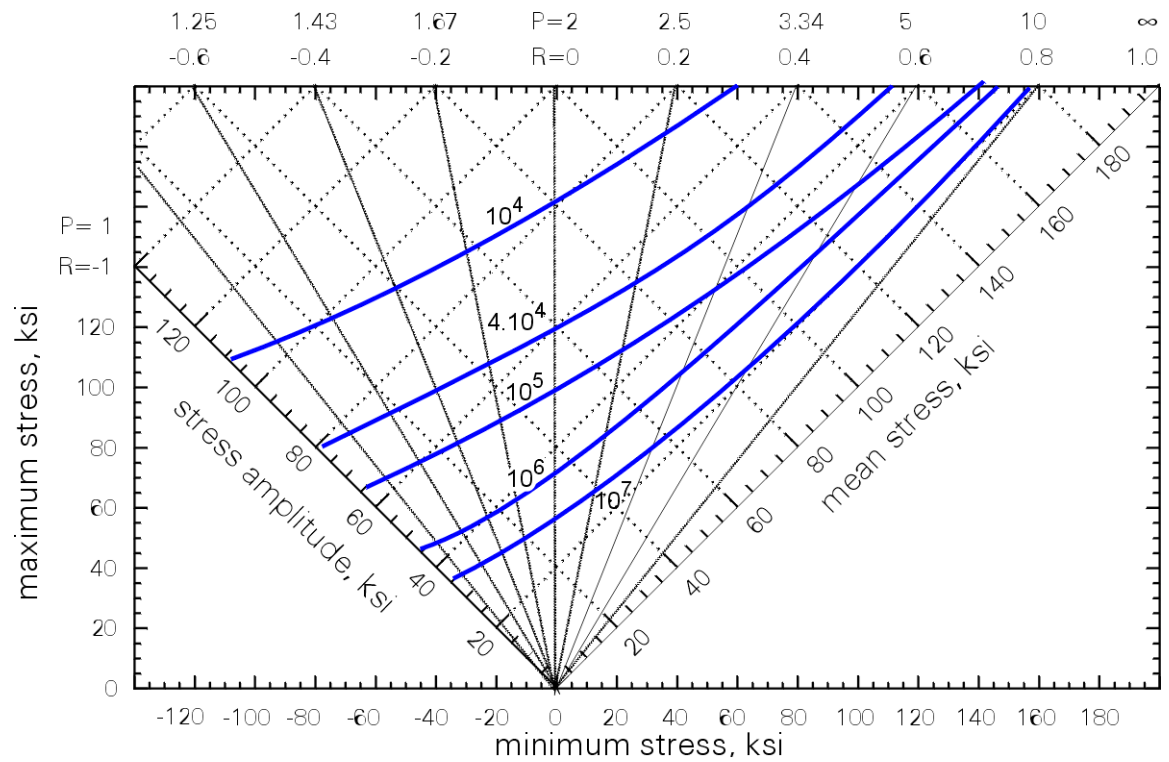


Fig. 10: The fatigue constant-life diagram for the V-ROL N steel (notched specimens,  
 $K_t = 2.0$ ) 1 ksi = 6.895 MPa.

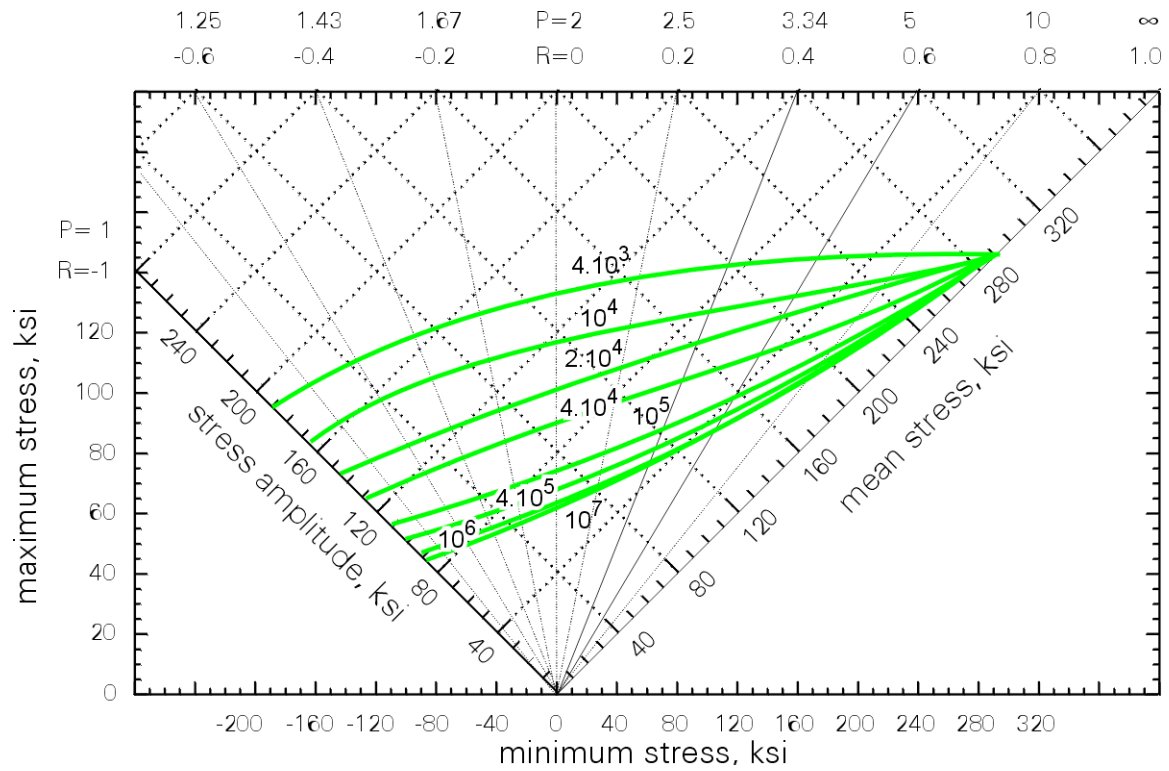


Fig. 11: The fatigue constant-life diagram for the 300M steel (smooth specimens)  
 1 ksi = 6.895 MPa.

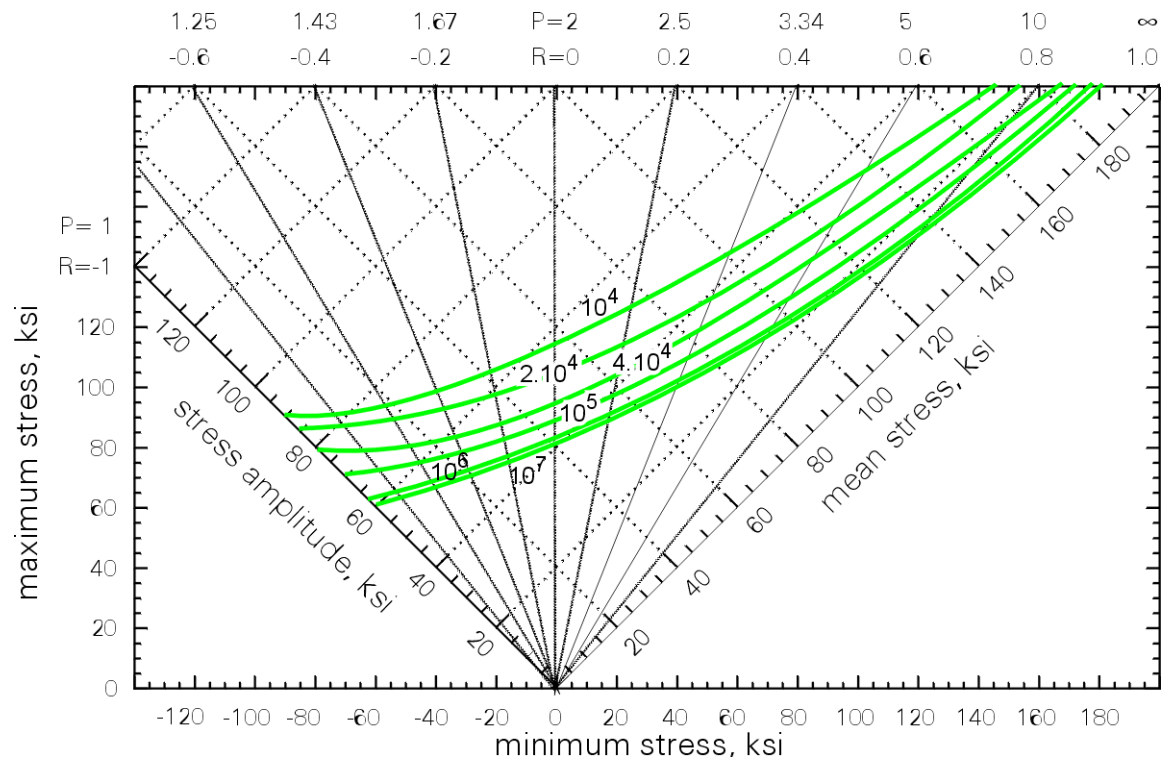


Fig. 12: The fatigue constant-life diagram for the 300M steel (notched specimens,  
 $K_t = 2.0$ ) 1 ksi = 6.895 MPa.



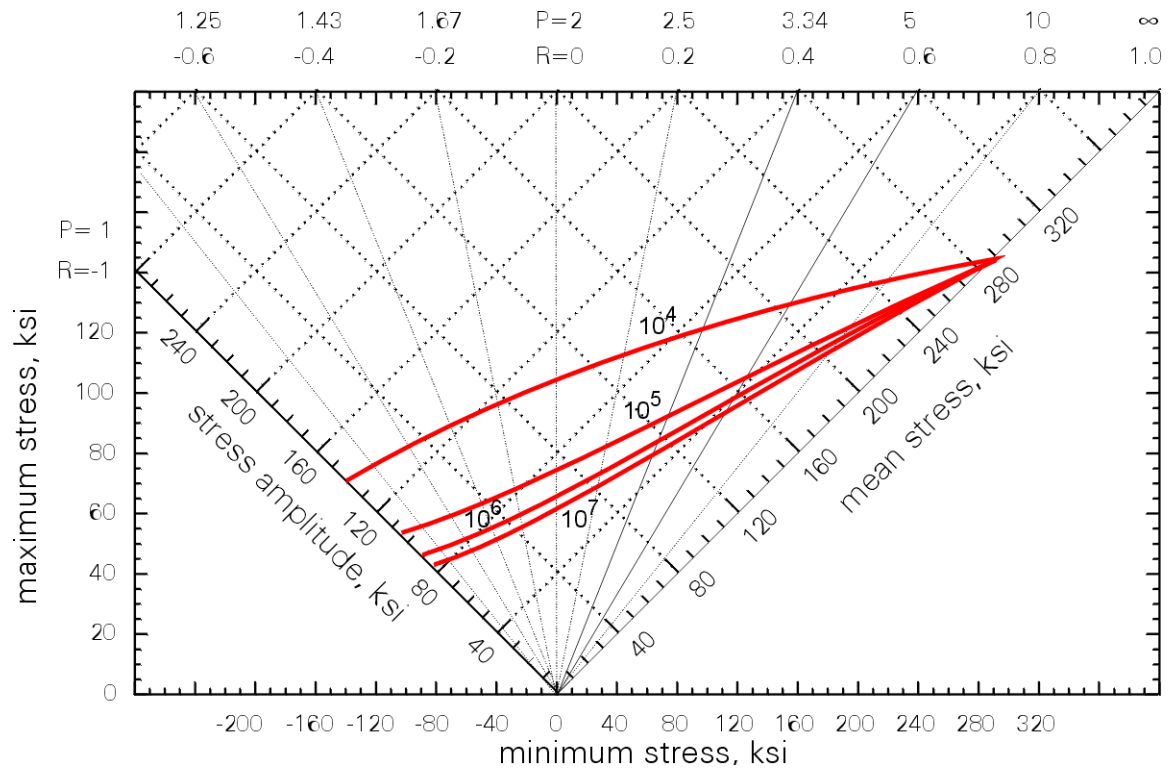


Fig. 13: The fatigue constant-life diagram for the P-LDHA steel (smooth specimens)  
1 ksi = 6.895 MPa.

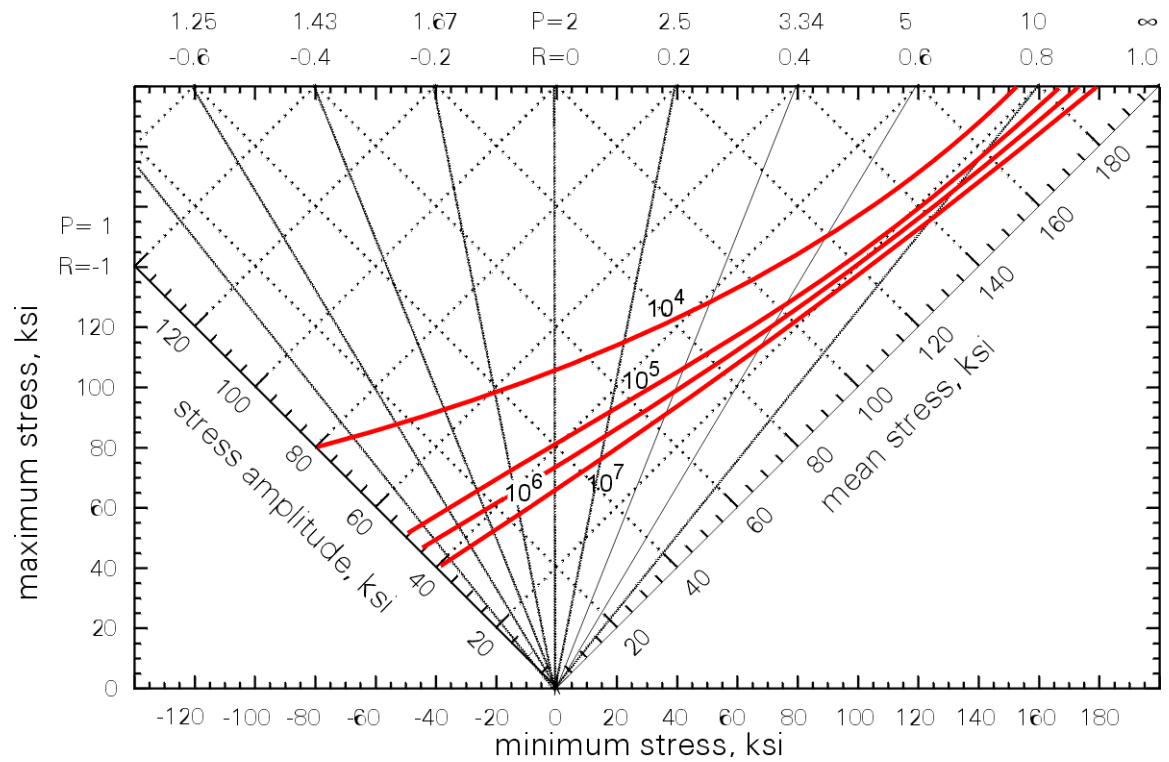


Fig. 14: The fatigue constant-life diagram for the P-LDHA steel (notched specimens,  
 $K_t = 2.3$ ) 1 ksi = 6.895 MPa.

Typical fatigue constant-life diagrams according to the standard MIL [5], including the influence of the mean stress ( $R = \sigma_{\min} / \sigma_{\max}$ ,  $P = \sigma_{\max} / \sigma_a$ ), are shown in Figs. 9, 11 and 13 (smooth specimens) and Figs. 10, 12 and 14 (notched specimens,  $K_t$  is the stress concentration factor) for selected UHSLA steels and the optimum tempering temperature of 300 °C. The stress in the diagrams is scaled in ksi units in order to allow a direct comparison with American standards MIL. In case of smooth specimens, the fatigue resistance of all steels is nearly comparable. In case of notched specimens, on the other hand, the V-ROL N steel exhibits the best resistance in the low-cycle region but the worst resistance in the high-cycle region (note the slightly higher  $K_t = 2.3$  in the tests of the P-LDHA steel).

An important property of UHSLA materials used for components exploited in the low cycle fatigue region is the resistance against the ratcheting (cyclic creep at the room temperature). As shown in [13, 14], the process can start only after reaching a characteristic value of the cyclic plastic deformation  $\varepsilon_{apth}$ . The dependences of this value (normalised to the ultimate strain  $\varepsilon_u$ ) on the cyclic ratio  $P$ , the so called ratcheting threshold curves, are shown in Fig. 15 for steels P-LDHA and V-ROL N and various tempering temperatures. As expected, the maximum resistance of the P-LDHA steel corresponds to  $T_t = 300$  °C. However, it is shifted down to 200 °C in case of the V-ROL N steel.

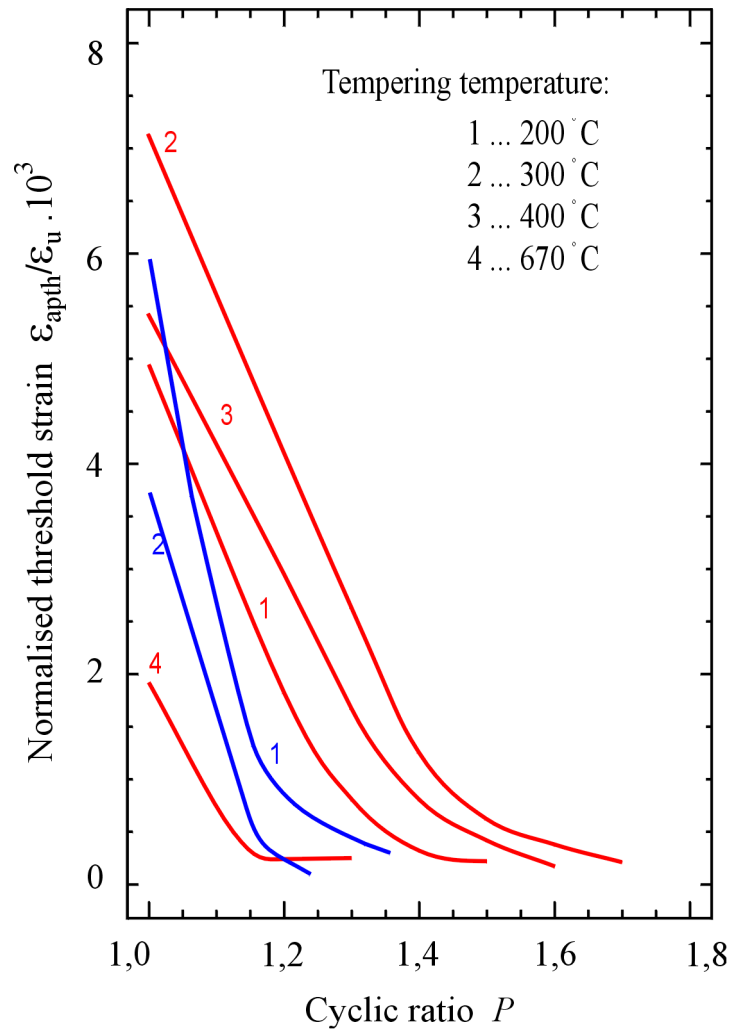


Fig. 15: Ratcheting threshold curves for steels P-LDHA (red) and V-ROL N (blue).

### 3. CONCLUSIONS

The investigation of the influence of the tempering temperature on mechanical properties of selected UHSLA steels, based on experiments on P-LDHA and V-ROL N steels and literature data for other steels, can be summarised in the following points:

- a) The optimum of tensile, toughness and fatigue characteristics corresponds to the tempering temperature of about 300 °C. In case of V-ROL N steel, however, the optimum of mechanical properties is shifted down to 200 °C.
- b) The mechanical properties of 300M and P-LDHA steels are, in average, better than those of AISI 4340, NiSiCr and V-ROL N steels.

### ACKNOWLEDGEMENT

This work was supported by the project MSM0021630518 of the Ministry of Education of the Czech Republic.

### REFERENCES

- 1) W. M. GARRISON, Jr., JOM, 42, 1990, p 20.
- 2) Y. TOMITA, Mat. Sci. Technology 7, 1991, p 481.
- 3) G. MALAKONDAIAH, M. SRINIVAS, P. RAMA RAO, Prog. Mat. Science 42, 1997, p 209.
- 4) J. POKLUDA, L. BARTÍK, P. ŠANDERA, in "Steels and Materials for Power Plants - Euromat 99" Ed. P. Neumann, D. Allen, E. Tenckhoff, Wiley-VCH, Weinheim, 2000, p 2022
- 5) Military Standardization Handbook, Metallic Materials and Elements for Aerospace Vehicle Structures, MIL-HDBK-5D, Department of Defence, USA 1983.
- 6) Military Standardization Handbook, Metallic Materials and Elements for Aerospace Vehicle Structures, MIL-HDBK-5G, Department of Defence, USA 1994.
- 7) GOST 4543-71
- 8) ČSN-ISO 41 6532
- 9) V. ŠAFEK et al., Research report VZÚ Poldi Kladno, a.s., Kladno 1992 (in Czech).
- 10) L. BARTÍK, PhD Thesis, Brno University of Technology, 1999.
- 11) R. M. HORN, R. O. RITCHIE, Metal. Trans., 9A, 1978, p. 1039.
- 12) S. K. BANERJI, C. J. MCMAHON Jr., H. C. FENG, Metal. Trans., 9A, 1978, p 237-247.
- 13) J. POKLUDA, P. STANĚK, Metal. Mater., 16, 1978, p 583.
- 14) J. POKLUDA, P. STANĚK, Scr. Met., 19, 1985, p 435.